# 基于一阶剪切板理论的FGM板刚柔耦合动力学建模与仿真*

杨兴[1,2†]　刘仁伟[1]　侯鹏[1]　章定国[2]

（1.上海卫星装备研究所，上海 200240）（2.南京理工大学 理学院，南京 210094）

**摘要**　对作大范围运动功能梯度材料（functionally graded materials，FGM）厚板的刚柔耦合动力学问题进行了研究，基于一阶剪切变形理论，从连续介质理论出发，计及了变形位移场中的二次耦合变形量，利用Lagrange方法推导了FGM厚板的刚柔耦合动力学方程，该方程适用于普通均质板和FGM板的动力学分析．采用20自由度矩形单元对变形场进行离散，对不同转速下的悬臂板进行动力学仿真，比较了本文建立的基于一阶剪切理论的模型和基于经典薄板理论的模型，验证了本文模型的正确性以及经典薄板理论的一些不足．研究了不同功能梯度指数下，FGM厚板的横向变形、速度响应频率和固有频率．结果表明，随着转速增大，剪切项对结构动力学行为影响变大；考虑横向剪切项的情况下，计算结果更偏柔性．

**关键词**　一阶剪切变形，　功能梯度材料，　有限元，　动力刚化

DOI：10.6052/1672-6553-2020-079

## 引言

近年来，随着航天航空器、能源动力、汽车工业、智能机器人等领域的蓬勃发展，力学与机械、材料、电子、生物等多学科的交叉不断加深，FGM的研究受到了更多重视．FGM[1,2]作为一种新兴的材料，其特殊的力学和物理性能使其在实际工程中有着广泛的应用前景，因此，对FGM的研究具有重要意义．自从Kane[3,4]揭示了动力刚化现象以来，国内外学者对梁、板结构的动力刚化问题进行了大量的研究[5-9]．Yoo[10]采用几何约束法对作大范围运动薄板的动力刚度项进行修正，采用假设模态法对变形场进行离散．赵飞云、洪嘉振等[11]基于连续介质力学理论，考虑了变形二次项，推导了高速旋转矩形柔性薄板的动力学方程．吴根勇、和兴锁等[12]基于经典薄板理论建立了大范围运动层合板的动力学方程，计入了传统建模方法忽略的二次耦合变形量，研究了铺层数与外侧角点变形的关系．黎亮、章定国[13,14]研究了大范围转动悬臂功能梯度矩形薄板的动力学问题，仿真了计及二次耦合变形量的功能梯度薄板作旋转的动力学行为．以上文献都是基于经典薄板理论进行研究，经典薄板理论是Kirchhoff于1850年发表的第一个完善的板弯曲理论．经典薄板理论要求板的厚度与边长之比处于薄板范围内．对于工程结构中大量使用的薄板问题，经典薄板理论能够给出满意精度的解．然而，对于中厚板，经典薄板理论的解不仅精度不高，甚至还会出现错误的结果．因此，国内外学者对中厚板建模理论[15]进行了研究．Sudhagar等[16]基于一阶剪切变形理论研究了一种复合材料板的受迫振动响应，对不同边界条件下复合材料板自由振动模态进行比较分析．李坦等[17]基于一阶剪切变形理论，利用余能原理，建立了一种高阶杂交应力六节点三角形Mindlin板单元，并且对四边简支中厚板的弯曲和振动进行数值仿真分析．Zhang等[18]研究了由碳纳米管增强的FGM三角形板的自由振动特性，考虑了板的横向剪切变形影响．Vu等[19]基于无网格方法分析了功能梯度薄板和中厚板的静态弯曲和自由振动问题．陈丽华等[20]基于Mindlin板理论对不同裂纹参数的悬臂板固有频率和模态进行了研究．现有文献大都是研究中厚板静力学问题，对作大范围运动的FGM厚板动力学研究比较少见．

2019-05-31 收到第1稿，2019-08-31 收到修改稿．

* 国家自然科学基金资助项目（11272155，11502113）和中央高校基本科研业务费专项基金（30917011103）

† 通讯作者 E-mail：115113001212@njust.edu.cn

## 1 柔性厚板运动学分析

作大范围旋转的功能梯度厚板如图1所示，坐标系 $O-XYZ$ 为惯性坐标系，$o-xyz$ 为连体坐标系，三个方向的单位矢量分别为 $\boldsymbol{a}_1$、$\boldsymbol{a}_2$、$\boldsymbol{a}_3$. 板的长度为 $a$，宽度为 $b$，厚度为 $h$，密度 $\rho(z)$，弹性模量为 $E(z)$，泊松比为 $\mu$. 变形前板中面上一点 $\mathrm{P}_0$（在连体坐标系下坐标为 $(x,y,z)$）变形后至P点.

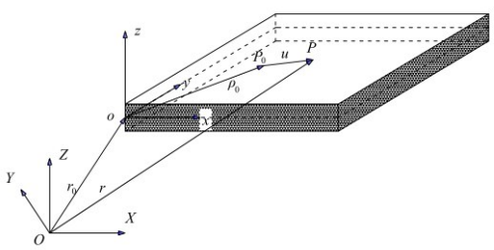


图1 作大范围运动功能梯度厚板

Fig.1 A functionally graded plate undergoing large motion

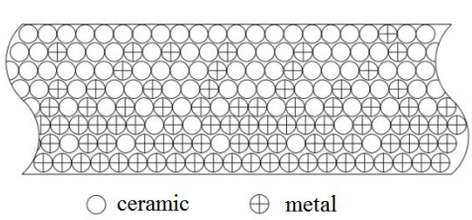


图2 板沿厚度方向材料分布

Fig.2 Distribution of material along the direction of thickness

根据一阶剪切变形理论和Von-Karman原理[15]，厚板上任意一点的变形位移和应变为：

$$\begin{cases} u_1 = w_1 \underline{-\dfrac{1}{2}\displaystyle\int_0^x \left(\frac{\partial u_3}{\partial \xi}\right)^2 \mathrm{d}\xi} + \underline{\underline{z\varphi_x}} \\ u_2 = w_2 \underline{-\dfrac{1}{2}\displaystyle\int_0^y \left(\frac{\partial u_3}{\partial \xi}\right)^2 \mathrm{d}\xi} + \underline{\underline{z\varphi_y}} \\ u_3 = u_3 \end{cases} \tag{1}$$

$$\begin{cases} \varepsilon_{11} = \dfrac{\partial w_1}{\partial x} + z\dfrac{\partial \varphi_x}{\partial x} \\ \varepsilon_{22} = \dfrac{\partial w_2}{\partial y} + z\dfrac{\partial \varphi_y}{\partial y} \\ \gamma_{12} \approx \dfrac{\partial w_1}{\partial y} + \dfrac{\partial w_2}{\partial x} + z\left(\dfrac{\partial \varphi_x}{\partial y} + \dfrac{\partial \varphi_y}{\partial x}\right) \\ \gamma_{13} = \dfrac{\partial u_3}{\partial x} + \varphi_x \\ \gamma_{23} = \dfrac{\partial u_3}{\partial y} + \varphi_y \end{cases} \tag{2}$$

厚板板内任意一点的变形位移矢量为 $u$，在连体坐标系下个分量为 $(u_1,u_2,u_3)$. 其中面内纵向拉伸变形位移 $u_1$，$u_2$ 可以用板中面 $(z=0)$ 上的变形表示. 式(1)中 $w_1-\dfrac{1}{2}\displaystyle\int_0^x \left(\frac{\partial u_3}{\partial \xi}\right)^2 \mathrm{d}\xi$ 和 $w_2-\dfrac{1}{2}\displaystyle\int_0^y \left(\frac{\partial u_3}{\partial \xi}\right)^2 \mathrm{d}\xi$ 分别为板中面上 $x$ 和 $y$ 方向上的变形，$w_1$ 和 $w_2$ 分别为板中面内沿 $x$ 和 $y$ 方向的实际伸长量，$\dfrac{1}{2}\displaystyle\int_0^x \left(\frac{\partial u_3}{\partial \xi}\right)^2 \mathrm{d}\xi$ 和 $\dfrac{1}{2}\displaystyle\int_0^y \left(\frac{\partial u_3}{\partial \xi}\right)^2 \mathrm{d}\xi$ 为二次耦合变形量. 传统的零次近似模型忽略了二次耦合变形量，即式(1)中单下划线项. $\varphi_x$、$\varphi_y$ 分别为柔性厚板中面法线相对于 $y$ 轴和 $x$ 轴的转角，基于经典薄板理论的变形场表达式中没有考虑横向剪切效应影响，即式(1)中的双下划线项.

本文所研究的FGM厚板由陶瓷和金属两种材料介质组成，板的弹性模量 $E(z)$ 和密度 $\rho(z)$ 沿板的厚度呈幂函数分布，表示为：

$$\begin{cases} E(z) = (E_{\mathrm{c}} - E_{\mathrm{m}})\left(\dfrac{2z+h}{2h}\right)^N + E_{\mathrm{m}} \\ \rho(z) = (\rho_{\mathrm{c}} - \rho_{\mathrm{m}})\left(\dfrac{2z+h}{2h}\right)^N + \rho_{\mathrm{m}} \end{cases} \tag{3}$$

其中，$N(N \geqslant 0)$ 为功能梯度指数，$h$ 为板厚度. 下标‘c’、‘m’分别代表陶瓷材料和金属材料. 泊松比 $\mu_{\mathrm{c}} = \mu_{\mathrm{m}} = \mu$. 板的长度为 $a$，宽度为 $b$，厚度为 $h$.

P点在惯性基下的速度矢量可表示为：

$$\boldsymbol{V}_P = \boldsymbol{V}_o + \boldsymbol{\omega}_A \times (\boldsymbol{\rho}_0 + \boldsymbol{u}) + \boldsymbol{V}_{PA} \tag{4}$$

上式中，$\boldsymbol{V}_o$、$\boldsymbol{\omega}_A$ 为连体坐标系相对于惯性坐标系的速度、角速度矢量，$\boldsymbol{\rho}_0$ 为点 $\mathrm{P}_0$ 在连体坐标系中位置矢量，$\boldsymbol{u}$ 为 $\mathrm{P}_0$ 的变形矢量，$\boldsymbol{V}_{PA}$ 为P点相对连体坐标系的速度矢量. 各矢量在连体坐标系的分量形式为：

$$\begin{cases} \boldsymbol{V}_o = v_1\boldsymbol{a}_1 + v_2\boldsymbol{a}_2 + v_3\boldsymbol{a}_3 \\ \boldsymbol{\omega}_A = \omega_1\boldsymbol{a}_1 + \omega_2\boldsymbol{a}_2 + \omega_3\boldsymbol{a}_3 \\ \boldsymbol{\rho}_0 = x\boldsymbol{a}_1 + y\boldsymbol{a}_2 + z\boldsymbol{a}_3 \\ \boldsymbol{u} = u_1\boldsymbol{a}_1 + u_2\boldsymbol{a}_2 + u_3\boldsymbol{a}_3 \\ \boldsymbol{V}_{PA} = \dot{u}_1\boldsymbol{a}_1 + \dot{u}_2\boldsymbol{a}_2 + \dot{u}_3\boldsymbol{a}_3 \end{cases} \tag{5}$$

将式(5)中各分量形代入式(4)，得到P点的速度表达式为：

$$\begin{aligned} \boldsymbol{V}_P = & \left[v_1 + \dot{u}_1 + \omega_2(u_3 + z) - \omega_3(y + u_2)\right]\boldsymbol{a}_1 \\ & + \left[v_2 + \dot{u}_2 + \omega_3(x + u_1) - \omega_1(u_3 + z)\right]\boldsymbol{a}_2 \\ & + \left[v_3 + \dot{u}_3 + \omega_1(y + u_2) - \omega_2(x + u_1)\right]\boldsymbol{a}_3 \end{aligned} \tag{6}$$

系统的动能为:

$$\begin{aligned}T&=\frac{1}{2}\int_V\rho(z)\boldsymbol{V}_P^{\mathrm{T}}\boldsymbol{V}_P\mathrm{d}V\\&=\frac{1}{2}\iiint_\Omega\rho(z)\Big[\left(v_1^2+v_2^2+v_3^2\right)+\left(\dot{u}_1^2+\dot{u}_2^2+\dot{u}_3^2\right)\\&\quad+\left(\dot{u}_1^2+\dot{u}_2^2+\dot{u}_3^2\right)+(\omega_1^2+\omega_2^2)(u_3+z)^2\\&\quad+(\omega_2^2+\omega_3^2)(x+u_1)^2+(\omega_1^2+\omega_3^2)(y+u_2)^2\\&\quad+(2v_1\dot{u}_1+2v_2\dot{u}_2+2v_3\dot{u}_3)\\&\quad+2(v_2\omega_3-v_3\omega_2)(x+u_1)+2(v_3\omega_1-v_1\omega_3)(y+u_2)\\&\quad+2(v_1\omega_2-v_2\omega_1)(u_3+z)+2\omega_2(u_3+z)\dot{u}_1\\&\quad-2\omega_3(y+u_2)\dot{u}_1+2\omega_3(x+u_1)\dot{u}_2\\&\quad-2\omega_1(u_3+z)\dot{u}_2+2\omega_1(y+u_2)\dot{u}_3\\&\quad-2\omega_2(x+u_1)\dot{u}_3-2\omega_2\omega_3(y+u_2)(u_3+\mathrm{z})\\&\quad-2\omega_1\omega_3(x+u_1)(u_3+\mathrm{z})\\&\quad-2\omega_1\omega_3(x+u_1)(y+u_2)\Big]\mathrm{d}V\end{aligned}\tag{7}$$

其中,$\rho(z)=(\rho_{\mathrm{c}}-\rho_{\mathrm{m}})(\frac{2z+h}{2h})^N+\rho_{\mathrm{m}}$

在板问题的研究中通常采用$\sigma_z=0$的假设,根据三维弹性理论,板内任意一点的应力为:

$$\begin{Bmatrix}\sigma_{11}\\\sigma_{22}\\\tau_{12}\\\tau_{13}\\\tau_{23}\end{Bmatrix}=\begin{bmatrix}C_{11}&C_{12}&0&0&0\\C_{12}&C_{22}&0&0&0\\0&0&C_{33}&0&0\\0&0&0&C_{44}&0\\0&0&0&0&C_{55}\end{bmatrix}\begin{Bmatrix}\varepsilon_{11}\\\varepsilon_{22}\\\gamma_{12}\\\gamma_{13}\\\gamma_{23}\end{Bmatrix}\tag{8}$$

其中$C_{11}$、$C_{12}$、$C_{22}$、$C_{33}$、$C_{44}$、$C_{55}$为板的材料参数.

$$C_{11}=\frac{E(z)}{1-\mu^2},C_{12}=\frac{\mu E(z)}{1-\mu^2},C_{22}=\frac{E(z)}{1-\mu^2},$$

$$C_{33}=\frac{E(z)}{2(1+\mu)},C_{44}=\frac{E(z)}{2(1+\mu)},C_{55}=\frac{E(z)}{2(1+\mu)}$$

系统的势能$U$分为两部分:板面内的变形能$U_m$,板弯曲和剪切变形能$U_b$.

$$\begin{aligned}U&=\frac{1}{2}\iiint_V(\sigma_{11}\varepsilon_{11}+\sigma_{22}\varepsilon_{22}+\tau_{12}\gamma_{12}+\tau_{23}\gamma_{23}+\tau_{13}\gamma_{13})\mathrm{d}V\\&=\frac{1}{2}\iiint_V\left\{\begin{array}{l}\dfrac{E(z)}{1-\mu^2}\left(\varepsilon_{11}^2+2\mu\varepsilon_{11}\varepsilon_{21}+\varepsilon_{22}^2+\dfrac{1-\mu}{2}\gamma_{12}^2\right.\\\qquad\left.+\dfrac{1-\mu}{2}\gamma_{23}^2+\dfrac{1-\mu}{2}\gamma_{13}^2\right)\end{array}\right\}\mathrm{d}V\\&=U_m+U_b\end{aligned}\tag{9}$$

$$\begin{aligned}U_m=\frac{1}{2}\iint_A\{&\frac{E_1}{1-\mu^2}\left[\left(\frac{\partial w_1}{\partial x}\right)^2+\left(\frac{\partial w_2}{\partial y}\right)^2+2\mu\left(\frac{\partial w_1}{\partial x}\right)\left(\frac{\partial w_2}{\partial y}\right)\right]\\&+\frac{E_1}{2(1+\mu)}\left(\frac{\partial w_1}{\partial y}+\frac{\partial w_2}{\partial x}\right)^2\}\mathrm{d}A\end{aligned}\tag{10}$$

$$\begin{aligned}U_b=&\frac{E_2}{2(1-\mu^2)}\iint_A\left\{\begin{array}{l}\left(\dfrac{\partial^2\varphi_x}{\partial x^2}\right)^2+\left(\dfrac{\partial^2\varphi_y}{\partial y^2}\right)^2\\+2\mu\left(\dfrac{\partial\varphi_x}{\partial x}\right)\left(\dfrac{\partial\varphi_y}{\partial y}\right)\\+\dfrac{1-\mu}{2}\left(\dfrac{\partial\varphi_x}{\partial y}+\dfrac{\partial\varphi_y}{\partial x}\right)^2\end{array}\right\}\mathrm{d}A\\&+\frac{E_1}{4(1+\mu)}\iint_A\left[\left(\frac{\partial u_3}{\partial x}+\varphi_x\right)^2+\left(\frac{\partial u_3}{\partial y}+\varphi_y\right)^2\right]\mathrm{d}A\end{aligned}\tag{11}$$

式(11)中,

$$E_1=\frac{E_c-E_m}{N+1}h+E_mh\tag{12}$$

$$\begin{aligned}E_2=&\left(E_c-E_m\right)h^3\left(\frac{1}{4(N+1)}-\frac{1}{(N+2)(N+3)}\right)\\&+\frac{E_mh^3}{12}\end{aligned}\tag{13}$$

## 2　柔性厚板变形场离散

本文采用20自由度矩形单元对变形场进行离散,矩形单元如图3所示:

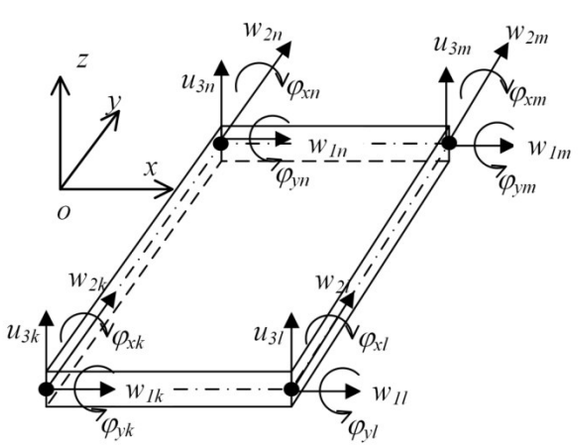


图3　4节点矩形单元

Fig.3　Four-node rectangular element

每个矩形单元有4个节点,每个节点有5个自由度,任意矩形j单元的自由度定义如下:

$$\begin{bmatrix}w_{1k}&w_{2k}&u_{3k}&\varphi_{xk}&\varphi_{yk}&w_{1l}&w_{2l}&u_{3l}&\varphi_{xl}&\varphi_{yl}\\w_{1m}&w_{2m}&u_{3m}&\varphi_{xm}&\varphi_{ym}&w_{1n}&w_{2n}&u_{3n}&\varphi_{xn}&\varphi_{yn}\end{bmatrix}$$

矩形厚板的变形场离散与矩形薄板不同,厚板要考虑到横向剪切变形,板中面法线相对于$y$轴的转角$\varphi_x$和相对于$x$轴的转角$\varphi_y$表示为独立变量.中厚板的变形场离散过程表示如下:

$$\begin{cases}\boldsymbol{w}_1(x,y,t)=\sum\limits_{i=1}^{4}\boldsymbol{\phi}_{1i}(x,y)\boldsymbol{q}_{1i}(t)=\boldsymbol{\Phi}_1(x,y)\boldsymbol{q}_1(t)\\ \boldsymbol{w}_2(x,y,t)=\sum\limits_{i=1}^{4}\boldsymbol{\phi}_{2i}(x,y)\boldsymbol{q}_{2i}(t)=\boldsymbol{\Phi}_2(x,y)\boldsymbol{q}_2(t)\\ \boldsymbol{u}_3(x,y,t)=\sum\limits_{i=1}^{4}\boldsymbol{\phi}_{3i}(x,y)\boldsymbol{q}_{3i}(t)=\boldsymbol{\Phi}_3(x,y)\boldsymbol{q}_3(t)\\ \boldsymbol{\varphi}_x(x,y,t)=\sum\limits_{i=1}^{4}\boldsymbol{\phi}_{4i}(x,y)\boldsymbol{q}_{3i}(t)=\boldsymbol{\phi}_4(x,y)\boldsymbol{q}_3(t)\\ \boldsymbol{\varphi}_y(x,y,t)=\sum\limits_{i=1}^{4}\boldsymbol{\phi}_{5i}(x,y)\boldsymbol{q}_{3i}(t)=\boldsymbol{\phi}_5(x,y)\boldsymbol{q}_3(t)\end{cases}\tag{14}$$

式（14）中，$\boldsymbol{\phi}_{1i}(x,y)$、$\boldsymbol{\phi}_{2i}(x,y)$、$\boldsymbol{\phi}_{3i}(x,y)$、$\boldsymbol{\phi}_{4i}(x,y)$、$\boldsymbol{\phi}_{5i}(x,y)$为单元内对应节点的形函数.$\boldsymbol{q}_1(t)\in\mathbf{R}^{N_1}$、$\boldsymbol{q}_2(t)\in\mathbf{R}^{N_2}$为相应节点面内纵向变形位移列阵，$\boldsymbol{q}_3(t)\in\mathbf{R}^{N_3}$为相应节点横向变形和截面转角组成的列阵.$u_3$和两个转角$\varphi_x$、$\varphi_y$的形函数行阵表示为：

$$\begin{aligned}&\boldsymbol{\phi}_{3i}=\begin{bmatrix}\phi_{3i} & 0 & 0\end{bmatrix}\\ &\boldsymbol{\phi}_{4i}=\begin{bmatrix}0 & \phi_{4i} & 0\end{bmatrix}\\ &\boldsymbol{\phi}_{5i}=\begin{bmatrix}0 & 0 & \phi_{5i}\end{bmatrix}\end{aligned}\tag{15}$$

$\boldsymbol{q}_{3i}(t)$表示为：

$$\boldsymbol{q}_{3i}(t)=\begin{bmatrix}u_{3i} & \varphi_{xi} & \varphi_{yi}\end{bmatrix}^{\mathrm{T}}\tag{16}$$

为了方便表述，下文的表达式中将略去自变量$x,y,t$.

令$\boldsymbol{\Phi}_4=z\boldsymbol{\phi}_4$，$\boldsymbol{\Phi}_5=z\boldsymbol{\phi}_5$，将式(14)代入式(1)，得变量$u_1,u_2,u_3$及其速度表达式：

$$\begin{cases}u_1=\boldsymbol{\Phi}_1\boldsymbol{q}_1-\dfrac{1}{2}\boldsymbol{q}_3^{\mathrm{T}}\boldsymbol{H}_1(x,y)\boldsymbol{q}_3+\boldsymbol{\Phi}_4\boldsymbol{q}_3\\ u_2=\boldsymbol{\Phi}_2\boldsymbol{q}_2-\dfrac{1}{2}\boldsymbol{q}_3^{\mathrm{T}}\boldsymbol{H}_2(x,y)\boldsymbol{q}_3+\boldsymbol{\Phi}_5\boldsymbol{q}_3\\ u_3=\boldsymbol{\Phi}_3\boldsymbol{q}_3\end{cases}\tag{17}$$

$$\begin{cases}\dot{u}_1=\boldsymbol{\Phi}_1\dot{\boldsymbol{q}}_1-\boldsymbol{q}_3^{\mathrm{T}}\boldsymbol{H}_1(x,y)\dot{\boldsymbol{q}}_3+\boldsymbol{\Phi}_4\dot{\boldsymbol{q}}_3\\ \dot{u}_2=\boldsymbol{\Phi}_2\dot{\boldsymbol{q}}_2-\boldsymbol{q}_3^{\mathrm{T}}\boldsymbol{H}_2(x,y)\dot{\boldsymbol{q}}_3+\boldsymbol{\Phi}_5\dot{\boldsymbol{q}}_3\\ \dot{u}_3=\boldsymbol{\Phi}_3\dot{\boldsymbol{q}}_3\end{cases}\tag{18}$$

对于有限元法，在$j$单元内，形函数的具体表达式如下：

$$\begin{aligned}&\boldsymbol{\phi}_{j1}=\boldsymbol{\phi}_{j2}=\begin{bmatrix}\psi_k & \psi_l & \psi_m & \psi_n\end{bmatrix}\\ &\psi_r=\frac{1}{4}\left(1+\varsigma_r\varsigma\right)\left(1+\eta_r\eta\right)(r=k,l,m,n)\\ &\boldsymbol{\phi}_{j3}=\boldsymbol{\phi}_{j4}=\boldsymbol{\phi}_{j5}=\begin{bmatrix}N_k & N_l & N_m & N_n\end{bmatrix}\\ &\boldsymbol{N}_r=\begin{bmatrix}N_r & N_{xr} & N_{yr}\end{bmatrix}(r=k,l,m,n)\end{aligned}\tag{19}$$

$$\begin{cases}N_r=\dfrac{1}{8}\left(1+\varsigma_r\varsigma\right)\left(1+\eta_r\eta\right)\left(2+\varsigma_r\varsigma+\eta_r\eta-\varsigma^2-\eta^2\right)\\ N_{xr}=-\dfrac{1}{8}d\eta_r\left(1+\varsigma_r\varsigma\right)\left(1+\eta_r\eta\right)\left(1-\eta^2\right)\\ N_{yr}=\dfrac{1}{8}c\varsigma_r\left(1+\varsigma_r\varsigma\right)\left(1+\eta_r\eta\right)\left(1-\varsigma^2\right)\end{cases}\tag{20}$$

式(20)中，

$$\begin{cases}\varsigma=\dfrac{x}{c},\varsigma_r=\dfrac{x_r}{c}\\ \eta=\dfrac{y}{d},\eta_r=\dfrac{y_r}{d}\end{cases}\quad(r=k,l,m,n)\tag{21}$$

式(21)相应的偏导数为：

$$\begin{cases}\dfrac{\partial}{\partial x}=\dfrac{\partial}{\partial\varsigma}\dfrac{1}{c}\\ \dfrac{\partial}{\partial y}=\dfrac{\partial}{\partial\eta}\dfrac{1}{d}\end{cases}$$

$$\begin{cases}\dfrac{\partial^2}{\partial x^2}=\dfrac{\partial^2}{\partial\varsigma^2}\dfrac{1}{c^2}\\ \dfrac{\partial^2}{\partial y^2}=\dfrac{\partial^2}{\partial\eta^2}\dfrac{1}{d^2}\\ 2\dfrac{\partial^2}{\partial x\partial y}=\dfrac{\partial^2}{\partial\varsigma\partial\eta}\dfrac{2}{cd}\end{cases}\tag{22}$$

单元节点的变形位移列阵表示为：

$$\begin{aligned}&\boldsymbol{q}_{j1}=\begin{bmatrix}w_{1k} & w_{1l} & w_{1m} & w_{1n}\end{bmatrix}^{\mathrm{T}}\\ &\boldsymbol{q}_{j2}=\begin{bmatrix}w_{2k} & w_{2l} & w_{2m} & w_{2n}\end{bmatrix}^{\mathrm{T}}\\ &\boldsymbol{q}_{j3}=\begin{bmatrix}u_{3k} & \varphi_{xk} & \varphi_{yk} & u_{3l}\\ & \varphi_{xl} & \varphi_{yl} & u_{3m} & \varphi_{xm}\\ & \varphi_{ym} & u_{3n} & \varphi_{xn} & \varphi_{yn}\end{bmatrix}^{\mathrm{T}}\end{aligned}\tag{23}$$

单元耦合形函数表示如下：

$$\begin{cases}\boldsymbol{H}_1(x,y)=\dfrac{1}{c^2}R_{j3}^{\mathrm{T}}\displaystyle\int_{-1}^{\varsigma}\boldsymbol{\phi}_{3,\varsigma}^{\mathrm{T}}\boldsymbol{\phi}_{3,\varsigma}\mathrm{d}\varsigma R_{j3}\\ \qquad\qquad+\displaystyle\sum_{i\in mP_0}\frac{1}{c^2}R_{i3}^{\mathrm{T}}\int_{-1}^{1}\boldsymbol{\phi}_{3,\varsigma}^{\mathrm{T}}\boldsymbol{\phi}_{3,\varsigma}\mathrm{d}\varsigma R_{i3}\\ \boldsymbol{H}_2(x,y)=\dfrac{1}{d^2}R_{j3}^{\mathrm{T}}\displaystyle\int_{-1}^{\eta}\boldsymbol{\phi}_{3,\eta}^{\mathrm{T}}\boldsymbol{\phi}_{3,\eta}\mathrm{d}\eta R_{j3}\\ \qquad\qquad+\displaystyle\sum_{i\in nP_0}\frac{1}{d^2}R_{i3}^{\mathrm{T}}\int_{-1}^{1}\boldsymbol{\phi}_{3,\eta}^{\mathrm{T}}\boldsymbol{\phi}_{3,\eta}\mathrm{d}\eta R_{i3}\end{cases}\tag{24}$$

式(24)中$R_{j3}$和$R_{i3}$为单元编号决定的定位矩阵，$c$和$d$分别为单元长度和宽度的二分之一，$mP_0$和$nP_0$分别表示这两条线段经过的单元的集合.下标中“,”表示对坐标求偏导.

## 3 柔性厚板动力学方程

取广义坐标$\boldsymbol{q}=[\boldsymbol{q}_1^{\mathrm{T}},\boldsymbol{q}_2^{\mathrm{T}},\boldsymbol{q}_3^{\mathrm{T}}]^{\mathrm{T}}$，将动能和势能代

入第二类Lagrange方程

$$\frac{\mathrm{d}}{\mathrm{d}t}\left(\frac{\partial T}{\partial \dot{\boldsymbol{q}}}\right)-\frac{\partial T}{\partial \boldsymbol{q}}+\frac{\partial U}{\partial \boldsymbol{q}}=0$$

得到FGM厚板的刚柔耦合动力学方程为:

$$\begin{bmatrix}\boldsymbol{M}_{11} & 0 & \boldsymbol{M}_{13}\\ 0 & \boldsymbol{M}_{22} & \boldsymbol{M}_{23}\\ \boldsymbol{M}_{31} & \boldsymbol{M}_{32} & \boldsymbol{M}_{33}\end{bmatrix}\begin{bmatrix}\ddot{\boldsymbol{q}}_1\\ \ddot{\boldsymbol{q}}_2\\ \ddot{\boldsymbol{q}}_3\end{bmatrix}+\begin{bmatrix}0 & \boldsymbol{G}_{12} & \boldsymbol{G}_{13}\\ \boldsymbol{G}_{21} & 0 & \boldsymbol{G}_{23}\\ \boldsymbol{G}_{31} & \boldsymbol{G}_{32} & \boldsymbol{G}_{33}\end{bmatrix}\begin{bmatrix}\dot{\boldsymbol{q}}_1\\ \dot{\boldsymbol{q}}_2\\ \dot{\boldsymbol{q}}_3\end{bmatrix}+\begin{bmatrix}\boldsymbol{K}_{11} & \boldsymbol{K}_{12} & \boldsymbol{K}_{13}\\ \boldsymbol{K}_{21} & \boldsymbol{K}_{22} & \boldsymbol{K}_{23}\\ \boldsymbol{K}_{31} & \boldsymbol{K}_{32} & \boldsymbol{K}_{33}\end{bmatrix}\begin{bmatrix}\boldsymbol{q}_1\\ \boldsymbol{q}_2\\ \boldsymbol{q}_3\end{bmatrix}=\begin{bmatrix}\boldsymbol{Q}_1\\ \boldsymbol{Q}_2\\ \boldsymbol{Q}_3\end{bmatrix}\tag{25}$$

式(25)中各个分块矩阵表达式为:

$$\boldsymbol{M}_{11}=\boldsymbol{W}_{11},\boldsymbol{M}_{22}=\boldsymbol{W}_{22},\boldsymbol{M}_{33}=\boldsymbol{W}_{33}+\boldsymbol{W}_{44}+\boldsymbol{W}_{55}$$

$$\boldsymbol{M}_{31}=\boldsymbol{M}_{13}^{\mathrm{T}}=\boldsymbol{W}_{41}$$

$$\boldsymbol{M}_{32}=\boldsymbol{M}_{23}^{\mathrm{T}}=\boldsymbol{W}_{52}$$

$$\boldsymbol{G}_{12}=-\boldsymbol{G}_{21}^{\mathrm{T}}=-2\omega_3\boldsymbol{W}_{12}$$

$$\boldsymbol{G}_{23}=-\boldsymbol{G}_{32}^{\mathrm{T}}=-2\omega_1\boldsymbol{W}_{23}$$

$$\boldsymbol{G}_{13}=-\boldsymbol{G}_{31}^{\mathrm{T}}=2\left(\omega_2\boldsymbol{W}_{13}-\omega_3\boldsymbol{W}_{15}\right)$$

$$\boldsymbol{G}_{33}=2\omega_2\left(\boldsymbol{W}_{43}-\boldsymbol{W}_{34}\right)+2\omega_2\left(\boldsymbol{W}_{54}-\boldsymbol{W}_{45}\right)+2\omega_2\left(\boldsymbol{W}_{35}-\boldsymbol{W}_{53}\right)$$

$$\boldsymbol{K}_{11}=\boldsymbol{K}_{f11}-(\omega_2^2+\omega_3^2)\boldsymbol{W}_{11}$$

$$\boldsymbol{K}_{12}=\boldsymbol{K}_{f12}+(\omega_1\omega_2-\dot{\omega}_3)\boldsymbol{W}_{12}$$

$$\boldsymbol{K}_{13}=(\omega_1\omega_3+\dot{\omega}_2)\boldsymbol{W}_{13}-\left(\omega_2^2+\omega_3^2\right)\boldsymbol{W}_{14}+(\omega_1\omega_2-\dot{\omega}_3)\boldsymbol{W}_{15}$$

$$\boldsymbol{K}_{21}=\boldsymbol{K}_{f21}+(\omega_1\omega_2+\dot{\omega}_3)\boldsymbol{W}_{21}$$

$$\boldsymbol{K}_{22}=\boldsymbol{K}_{f22}-(\omega_1^2+\omega_3^2)\boldsymbol{W}_{22}$$

$$\boldsymbol{K}_{23}=(\omega_2\omega_3-\dot{\omega}_1)\boldsymbol{W}_{23}+\left(\dot{\omega}_3+\omega_1\omega_2\right)\boldsymbol{W}_{24}-\left(\omega_1^2+\omega_3^2\right)\boldsymbol{W}_{25}$$

$$\boldsymbol{K}_{31}=(\omega_1\omega_3-\dot{\omega}_2)\boldsymbol{W}_{31}-\left(\omega_2^2+\omega_3^2\right)\boldsymbol{W}_{41}+\left(\dot{\omega}_3+\omega_1\omega_2\right)\boldsymbol{W}_{51}$$

$$\boldsymbol{K}_{32}=(\omega_2\omega_3+\dot{\omega}_1)\boldsymbol{W}_{32}+\left(\omega_1\omega_2-\dot{\omega}_3\right)\boldsymbol{W}_{42}-\left(\omega_1^2+\omega_3^2\right)\boldsymbol{W}_{52}$$

$$\boldsymbol{K}_{33}=\boldsymbol{K}_{f33}-(\omega_1^2+\omega_2^2)\boldsymbol{W}_{33}-\left(\omega_2^2+\omega_3^2\right)\boldsymbol{W}_{44}-(\omega_1^2+\omega_3^2)\boldsymbol{W}_{55}-\dot{\omega}_2\boldsymbol{W}_{34}+\dot{\omega}_1\boldsymbol{W}_{35}+\left(2\omega_1\omega_3+\dot{\omega}_2\right)\boldsymbol{W}_{43}+\left(2\omega_1\omega_2-\dot{\omega}_3\right)\boldsymbol{W}_{45}+\left(2\omega_2\omega_3-\dot{\omega}_1\right)\boldsymbol{W}_{54}+(\omega_2^2+\omega_3^2)\boldsymbol{D}_{11}+(\omega_1^2+\omega_3^2)\boldsymbol{D}_{22}-(\omega_1\omega_2+\dot{\omega}_3)\boldsymbol{D}_{12}-(\omega_1\omega_2-\dot{\omega}_3)\boldsymbol{D}_{21}-a_{01}\boldsymbol{C}_1-a_{02}\boldsymbol{C}_2$$

$$\boldsymbol{Q}_1=(\omega_2^2+\omega_3^2)\boldsymbol{S}_{11}^{\mathrm{T}}-(\omega_1\omega_2-\dot{\omega}_3)\boldsymbol{S}_{21}^{\mathrm{T}}-a_{01}\boldsymbol{Y}_1^{\mathrm{T}}$$

$$\boldsymbol{Q}_2=(\omega_1^2+\omega_3^2)\boldsymbol{S}_{22}^{\mathrm{T}}-(\omega_1\omega_2+\dot{\omega}_3)\boldsymbol{S}_{12}^{\mathrm{T}}-a_{02}\boldsymbol{Y}_2^{\mathrm{T}}$$

$$\boldsymbol{Q}_3=-(\omega_1\omega_3-\dot{\omega}_2)\boldsymbol{S}_{13}^{\mathrm{T}}+\left(\omega_2^2+\omega_3^2\right)\boldsymbol{S}_{14}^{\mathrm{T}}-\left(\omega_1\omega_2+\dot{\omega}_3\right)\boldsymbol{S}_{15}^{\mathrm{T}}-(\omega_2\omega_3+\dot{\omega}_1)\boldsymbol{S}_{23}^{\mathrm{T}}-(\omega_1\omega_2-\dot{\omega}_3)\boldsymbol{S}_{24}^{\mathrm{T}}+\left(\omega_1^2+\omega_3^2\right)\boldsymbol{S}_{25}^{\mathrm{T}}-a_{03}\boldsymbol{Y}_3^{\mathrm{T}}-a_{01}\boldsymbol{Y}_4^{\mathrm{T}}-a_{02}\boldsymbol{Y}_5^{\mathrm{T}}-\dot{\omega}_2\boldsymbol{S}_{34}^{\mathrm{T}}-\omega_2\omega_3\boldsymbol{S}_{35}^{\mathrm{T}}\tag{26}$$

$\boldsymbol{K}_{33}$表达式中$a_{01}$、$a_{02}$、$a_{03}$为基点加速度在浮动基下的分量:

$$\begin{aligned}\boldsymbol{a}_{01}&=\dot{v}_1+\left(\omega_2v_3-\omega_3v_2\right)\\ \boldsymbol{a}_{02}&=\dot{v}_2+\left(\omega_3v_1-\omega_1v_3\right)\\ \boldsymbol{a}_{03}&=\dot{v}_3+\left(\omega_1v_2-\omega_2v_1\right)\end{aligned}\tag{27}$$

式(26)中各常数阵为:

$$\boldsymbol{W}_{ij}=\iiint_V\boldsymbol{\rho}(z)\boldsymbol{\phi}_i^{\mathrm{T}}\boldsymbol{\phi}_j\,\mathrm{d}V\quad\left(i=1,2,3,4,5\quad j=1,2,3,4,5\right)$$

$$\boldsymbol{C}_i=\iiint_V\rho(z)\cdot\boldsymbol{H}_i\mathrm{d}V\quad(i=1,2)$$

$$\boldsymbol{D}_{1i}=\iiint_V\rho(z)\cdot x\cdot\boldsymbol{H}_i\mathrm{d}V\quad(i=1,2)$$

$$\boldsymbol{D}_{2i}=\iiint_V\rho(z)\cdot y\cdot\boldsymbol{H}_i\mathrm{d}V\quad(i=1,2)$$

$$\boldsymbol{S}_{1i}=\iiint_V\rho(z)\cdot x\cdot\boldsymbol{\phi}_i\,\mathrm{d}V\quad(i=1,2,3,4,5)$$

$$\boldsymbol{S}_{2i}=\iiint_V\rho(z)\cdot y\cdot\boldsymbol{\phi}_i\,\mathrm{d}V\quad(i=1,2,3,4,5)$$

$$\boldsymbol{S}_{3i}=\iiint_V\rho(z)\cdot z\cdot\boldsymbol{\phi}_i\,\mathrm{d}V\quad(i=1,2,3,4,5)$$

$$\boldsymbol{Y}_i=\iiint_V\rho(z)\cdot\boldsymbol{\phi}_i\,\mathrm{d}V\quad(i=1,2,3,4,5)$$

$$\boldsymbol{K}_{f11}=\iiint_V\frac{E(z)}{1-\mu^2}\left(\boldsymbol{\phi}_{1,x}^{\mathrm{T}}\boldsymbol{\phi}_{1,x}+\frac{1-\mu}{2}\boldsymbol{\phi}_{1,y}^{\mathrm{T}}\boldsymbol{\phi}_{1,y}\right)\mathrm{d}V$$

$$\boldsymbol{K}_{f12}=\boldsymbol{K}_{f21}^{\mathrm{T}}=\iiint_V\frac{E(z)}{1-\mu^2}\left(\mu\boldsymbol{\phi}_{1,x}^{\mathrm{T}}\boldsymbol{\phi}_{2,y}+\frac{1-\mu}{2}\boldsymbol{\phi}_{1,y}^{\mathrm{T}}\boldsymbol{\phi}_{2,x}\right)\mathrm{d}V$$

$$\boldsymbol{K}_{f22}=\iiint_V\frac{E(z)}{1-\mu^2}\left(\boldsymbol{\phi}_{2,y}^{\mathrm{T}}\boldsymbol{\phi}_{2,y}+\frac{1-\mu}{2}\boldsymbol{\phi}_{2,x}^{\mathrm{T}}\boldsymbol{\phi}_{2,x}\right)\mathrm{d}V$$

$$\boldsymbol{K}_{f33}=K_{f_1 33}+K_{f_2 33}$$

$$\boldsymbol{K}_{f_1 33}=\iiint_V\frac{E(z)}{12(1-\mu^2)}\left[\boldsymbol{\phi}_{4,x}^{\mathrm{T}}\boldsymbol{\phi}_{4,x}+\boldsymbol{\phi}_{5,y}^{\mathrm{T}}\boldsymbol{\phi}_{5,y}+\boldsymbol{\mu}\left(\boldsymbol{\phi}_{4,x}^{\mathrm{T}}\boldsymbol{\phi}_{5,y}+\boldsymbol{\phi}_{5,y}^{\mathrm{T}}\boldsymbol{\phi}_{4,x}\right)+\frac{1-\boldsymbol{\mu}}{2}\left(\boldsymbol{\phi}_{4,y}^{\mathrm{T}}\boldsymbol{\phi}_{4,y}+\boldsymbol{\phi}_{5,x}^{\mathrm{T}}\boldsymbol{\phi}_{5,x}+\boldsymbol{\phi}_{4,y}^{\mathrm{T}}\boldsymbol{\phi}_{5,x}+\boldsymbol{\phi}_{5,x}^{\mathrm{T}}\boldsymbol{\phi}_{4,y}\right)\right]\mathrm{d}V$$

$$\boldsymbol{K}_{f_2 33}=\iiint_V\frac{E(z)}{2\left(1+\boldsymbol{\mu}\right)}\left[\boldsymbol{\phi}_{3,x}^{\mathrm{T}}\boldsymbol{\phi}_{3,x}+\boldsymbol{\phi}_{3,y}^{\mathrm{T}}\boldsymbol{\phi}_{3,y}+\boldsymbol{\phi}_4^{\mathrm{T}}\boldsymbol{\phi}_4+\boldsymbol{\phi}_5^{\mathrm{T}}\boldsymbol{\phi}_5+\boldsymbol{\phi}_{3,x}^{\mathrm{T}}\boldsymbol{\phi}+\boldsymbol{\phi}_4^{\mathrm{T}}\boldsymbol{\phi}_{3,x}+\boldsymbol{\phi}_{3,y}^{\mathrm{T}}\boldsymbol{\phi}_5+\boldsymbol{\phi}_5^{\mathrm{T}}\boldsymbol{\phi}_{3,y}\right]\mathrm{d}V\tag{28}$$

方程(25)可以模拟FGM柔性厚板的动力学问

题.式(26)中$K_{33}$项表达式中双下划线项为考虑二次耦合变形量而推导出的附加动力刚度项,若忽略这些项,则动力学方程退化为传统的零次模型.式(26)中单下划线项为考虑横向剪切变形效应推导出的项,若忽略剪切变形项,则动力学方程退化为传统经典薄板理论模型.式(28)中的$\rho(z)$、$E(z)$为FGM厚板的材料分布函数.

## 4 数值仿真

### 4.1 作定轴转动矩形板动力刚化研究

仿真作大范围运动悬臂功能梯度板的动力学行为,采用上文所述离散方法,将板离散为12×12个单元,中心刚体与板的一边固连,中心刚体以角速度$\omega$绕$y$轴旋转,中心刚体半径$R$=0,角速度$\omega_1$=$\omega_3$=0,$\omega_2$=$\omega$,角加速度$\dot{\omega}_1=\dot{\omega}_3=0$,$\dot{\omega}_2=\dot{\omega}$.

给定的角速度规律为:

$$\omega=\begin{cases}\dfrac{\Omega}{T}t-\dfrac{\Omega}{2\pi}\sin\left(\dfrac{2\pi}{T}t\right) & 0\leqslant t\leqslant T\\ \Omega & t>T\end{cases} \tag{29}$$

式(29)中,$T$=30s.

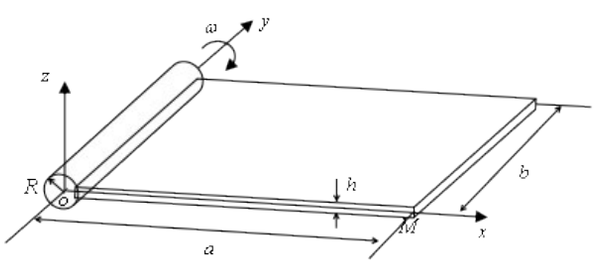


图4 绕中心刚体旋转的功能梯度板

Fig.4 A rotating cantilever functionally graded plate

只考虑板沿厚度方向上的横向振动,系统的动力学方程可以简化为:

$$\boldsymbol{M}_{33}\ddot{\boldsymbol{q}}_3+\boldsymbol{G}_{33}\dot{\boldsymbol{q}}_3+\boldsymbol{K}_{33}\boldsymbol{q}_3=\boldsymbol{Q}_3 \tag{30}$$

上式中各矩阵表达式已在上文中给出.

算例1.普通均质材料板参数:$a$=1.8828m,$b$=1.2192m,$h$=0.00254m,$E$=70GPa,$\rho$=2000kg/m$^3$,$\mu$=0.3.

算例2.FGM板的材料参数:$a$=1.8828m,$b$=1.2192m,$h$=0.1m,$E_c$=151GPa,$E_m$=70GPa,$\rho_c$=3000kg/m$^3$,$\rho_m$=2707kg/m$^3$,$\mu$=0.3.

算例1数值仿真:

图5-8为Ω=0.2Hz、Ω=0.275Hz、Ω=10Hz和Ω=20Hz时使用不同方法获得的模型外侧角点横向变形和横向变形速度.三种方法都计及了变形二次项,其中假设模态法和有限元法(finite element method,FEM)基于经典薄板理论,本文方法是基于一阶剪切变形理论,用20自由度矩形单元离散变形场,采用Newmark法数值求解,数值阻尼的存在使匀速转动阶段的横向变形逐渐减小.从图5和图6可以看出,各方法的仿真结果基本一致,这也验证了本文方法的正确性.从图6(b)匀速转动阶段的局部放大图可以看出,Ω=0.275Hz时基于经典薄板理论的有限元方法振幅最小,基于一阶剪切变形理论的本文方法振幅偏大,但是这个差异是很小的,都能满足实际工程要求.

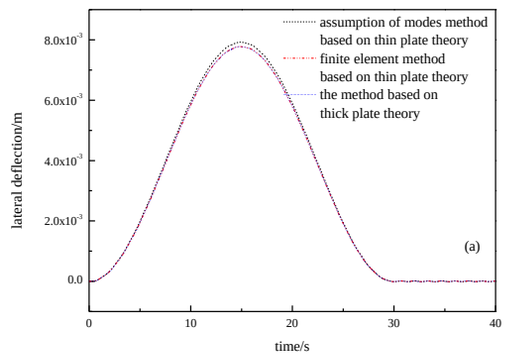


(a) 外侧角点横向变形

(a) Lateral deflection of the plate's corner

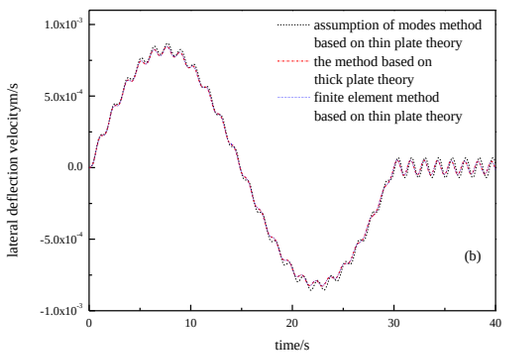


(b) 外侧角点横向变形速度

(b) Lateral deflection velocity of the plate's corner

图5 Ω = 0.2Hz时均质材料板数值仿真结果

Fig.5 Numerical simulation results of homogeneous material plates for the case of Ω = 0.2Hz

从图6(b)、图7(b)和图8(b)外侧角点变形放大图可以看出,转速恒定时,基于本文厚板理论模型得到的振幅和响应周期都比基于经典薄板理论的有限元法偏大一点,而且随着Ω的增大,这种差异越来越明显.这说明了经典薄板理论模型的计算结果使结构更偏刚性,在中心刚体转速提高时,计入了横向剪切变形效应的本文模型在描述大范围

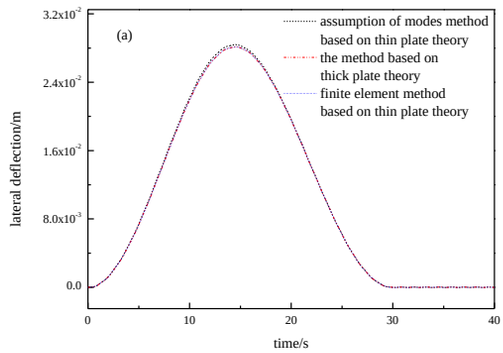


(a)外侧角点横向变形

(a)Lateral deflection of the plate's corner

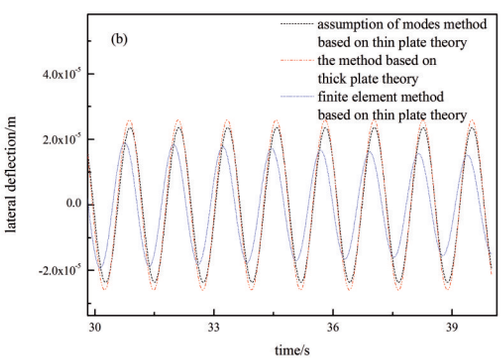


(b)匀速转动阶段放大图

(b)Enlarged view of uniform rotation stage

图6　Ω = 0.75Hz时均质材料板数值仿真结果

Fig.6　Numerical simulation results of homogeneous material plates for the case of Ω = 0.75Hz

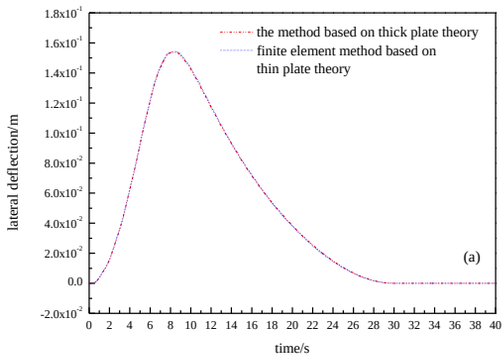


(a)外侧角点横向变形

(a)Lateral deflection of the plate's corner

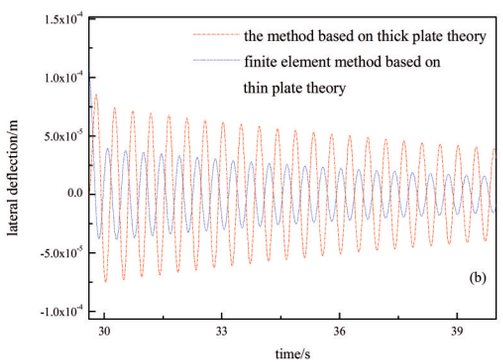


(b)匀速转动阶段放大图

(b)Enlarged view of uniform rotation stage

图7　Ω = 10Hz时均质材料板数值仿真结果

Fig.7　Numerical simulation results of homogeneous material plates for the case of Ω = 10Hz

运动板的动力学行为时更加准确.

算例2仿真:

对 $h = 0.1\text{m}$, $\Omega = 50\text{Hz}$ 的FGM厚板进行数值仿真.从图9(a)可以看出,随着N的增大,FGM厚板的外侧角点最大变形逐渐增大,匀速转动阶段的振幅也逐渐增大,这说明板的柔性是随着功能梯度指数N的增大而变大的.图9(c)为匀速转动阶段外侧角点横向变形速度放大图,由图可得功能梯度指数N越大,结构的速度响应周期也越长.

### 4.2　作定轴转动功能梯度矩形板固有频率研究

本节基于厚板理论和经典薄板理论对作匀速转动矩形板的横向弯曲固有频率进行研究.在只考虑板横向弯曲的情况下,得到基于厚板理论的FGM板振动方程为:

$$\boldsymbol{M}_{33}\ddot{\boldsymbol{q}}_3 + \left[\Omega^2\left(R\boldsymbol{C}_1 + \boldsymbol{D}_{11}\right) - \Omega^2\left(\boldsymbol{W}_{33} + \boldsymbol{W}_{44} + \boldsymbol{W}_{55}\right) + \boldsymbol{K}_{f_1 33} + \boldsymbol{K}_{f_2 33}\right]\boldsymbol{q}_3 = 0 \tag{31}$$

对式(31)进行无量纲化处理,引入以下无量纲变量:

$$\kappa = \frac{E_c}{E_m}, \chi = \frac{\rho_c}{\rho_m}, \delta = \frac{a}{b}, \tau = \frac{h}{a}, \sigma = \frac{R}{a},$$

$$\gamma = \Omega\left(\frac{12\rho_m h a^4\left(1-\mu^2\right)}{E_m}\right)^{1/2},$$

$$\varpi = \omega\left(\frac{12\rho_m h a^4\left(1-\mu^2\right)}{E_m}\right)^{1/2} \tag{32}$$

将式(32)代入式(31)可得无量纲形式振动方程:

$$\overline{\boldsymbol{M}}_{33}\ddot{\boldsymbol{q}}_3 + \left[\gamma^2\left(\sigma\,\overline{\boldsymbol{C}}_1 + \overline{\boldsymbol{D}}_{11} - \overline{\boldsymbol{W}}_{33} - \overline{\boldsymbol{W}}_{44} - \overline{\boldsymbol{W}}_{55}\right) + \zeta_1\overline{\boldsymbol{K}}_{f_1 33} + \zeta_2\overline{\boldsymbol{K}}_{f_2 33}\right]\boldsymbol{q}_3 = 0 \tag{33}$$

式(33)中 $\zeta_1$ 和 $\zeta_2$ 是与功能梯度指数N有关的FGM沿板厚度方向的分布系数,分别表示为:

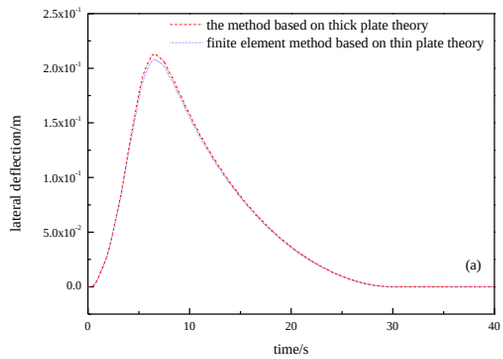


(a)外侧角点横向变形

(a)Lateral deflection of the plate's corner

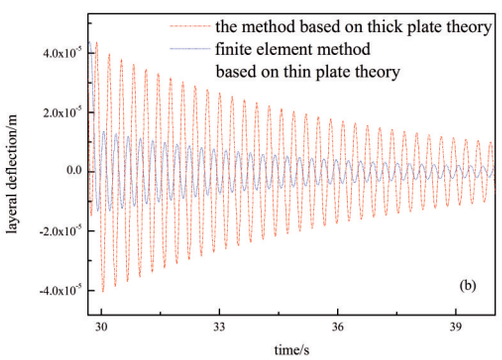


(b)匀速转动阶段放大图

(b)Enlarged view of uniform rotation stage

图 8 Ω = 20Hz 时均质材料板数值仿真结果

Fig.8 Numerical simulation results of homogeneous material plates for the case of Ω = 20Hz

$$\zeta_1 = (\kappa - 1)\frac{3(N^2 + N + 2)}{(N + \chi)(N + 2)(N + 3)} + \frac{N + 1}{N + \chi}$$

$$\zeta_2 = \frac{\kappa - N}{\chi + N} \tag{34}$$

将 FGM 板退化为普通均质板，表 1 和表 2 分别是 $\sigma = 0$ 和 $\sigma = 1$ 时悬臂板的前五阶无量纲固有频率($N = 0, \delta = 1, \tau = 0.01$). 文献[21]基于经典薄板理论，采用 5 × 7 阶的假设模态法. 基于经典薄板理论的有限元方法和基于本文建模理论的方法离散单元数均为 12 × 12，其中厚板理论采用第三章中所给的单元. 由表 1 和表 2 可知，在 $\gamma$ 相同的情况下，悬臂板的各阶无量纲固有频率中，基于经典薄板理论的假设模态法计算结果最大，这说明了假设模态法比有限元方法偏刚性. 基于本文厚板建模理论的计算结果小于基于经典薄板理论的假设模态法和有限元法，这是由于考虑了横向剪切变形的影响，悬臂板的柔性更大. 比较 $\sigma = 0$ 和 $\sigma = 1$ 的各阶无量纲固有频率可以发现，中心刚体半径的增大，悬臂板的无量纲固有频率也会增大. 表 3 是 N 取不同值时得到的旋转功能梯度厚板的前五阶无量纲固有频率，结果表明随着 N 的增加，功能梯度厚板的无量纲固有频率是降低的，N 的变化对高阶频率影响较大.

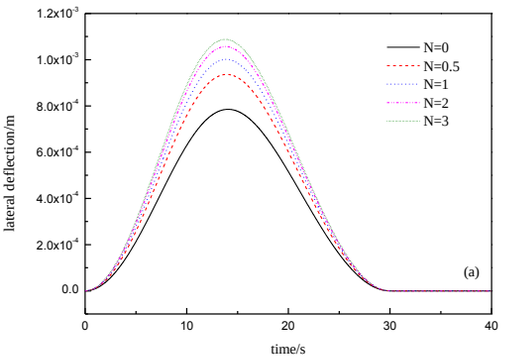


(a) 外侧角点横向变形

(a) Lateral deflection of the plate's corner

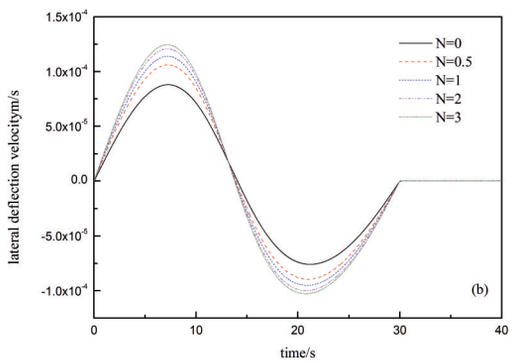


(b) 外侧角点横向变形速度

(b) Lateral deflection velocity of the plate's corner

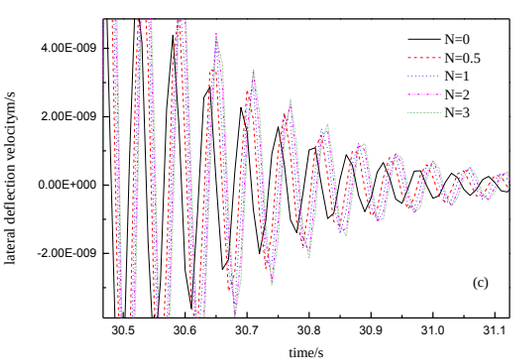


(c) 匀速转动阶段放大图

(c) Enlarged view of uniform rotation stage

图 9 Ω = 50Hz 时功能梯度厚板数值仿真结果

Fig.9 Numerical simulation results of functionally graded thick plates for the case of Ω = 50Hz

表 1　作定轴转动中心刚体-悬臂板的前五阶无量纲固有频率

Table 1　Five lowest dimensionless natural frequencies of a rotating cantilever plate $(\delta = 1,\tau = 0.01,\sigma = 0)$

| Dimensionless angular velocity | Frequency order | FEM based on thin plate theory | Thick plate theory | Reference [21] |
|---|---|---|---|---|
| $\gamma = 1$ | 1 | 3.498 | 3.496 | 3.516 |
| | 2 | 8.511 | 8.473 | 8.533 |
| | 3 | 21.468 | 21.320 | 21.520 |
| | 4 | 27.153 | 27.051 | 27.353 |
| | 5 | 31.049 | 30.836 | 31.206 |
| $\gamma = 2$ | 1 | 3.575 | 3.575 | 3.5963 |
| | 2 | 8.815 | 8.769 | 8.5507 |
| | 3 | 21.789 | 21.620 | 21.865 |
| | 4 | 27.176 | 27.025 | 27.384 |
| | 5 | 31.302 | 31.053 | 31.477 |

表 2　作定轴转动中心刚体-悬臂板的前五阶无量纲固有频率

Table 2　Five lowest dimensionless natural frequencies of a rotating cantilever plate $(\delta = 1,\tau = 0.01,\sigma = 1)$

| Dimensionless angular velocity | Frequency order | FEM based on thin plate theory | Thick plate theory | Reference [21] |
|---|---|---|---|---|
| $\gamma = 1$ | 1 | 3.715 | 3.7124 | 3.732 |
| | 2 | 8.598 | 8.5844 | 8.624 |
| | 3 | 21.645 | 21.472 | 21.706 |
| | 4 | 27.192 | 27.087 | 27.394 |
| | 5 | 31.186 | 30.724 | 31.350 |
| $\gamma = 2$ | 1 | 4.359 | 4.352 | 4.381 |
| | 2 | 8.854 | 8.816 | 8.909 |
| | 3 | 22.481 | 22.315 | 22.580 |
| | 4 | 27.342 | 27.201 | 27.557 |
| | 5 | 31.839 | 31.602 | 32.043 |

表 3　作定轴转动中心刚体-悬臂板的前五阶无量纲固有频率

Table 3　Five lowest dimensionless natural frequencies of a rotating cantilever functionally graded thick plate $(\gamma = 10,\delta = 1,\tau = 0.1,\sigma = 0)$

| Frequency order | N=1 | N=2 | N=3 | N=4 |
|---|---|---|---|---|
| 1 | 6.156 | 6.002 | 5.873 | 5.741 |
| 2 | 11.028 | 10.708 | 10.340 | 10.141 |
| 3 | 32.378 | 31.432 | 30.487 | 29.542 |
| 4 | 38.299 | 37.183 | 36.086 | 34.976 |
| 5 | 47.013 | 45.582 | 44.152 | 42.723 |

## 5　结论

本文基于一阶剪切变形理论,运用Lagrange方程,建立了作大范围运动功能梯度厚板的刚柔耦合动力学模型,建模过程中计及了传统建模方法忽略的二次耦合变形量,考虑了经典薄板理论模型忽略的横向剪切变形项,采用20自由度矩形单元对变形场进行离散.对不同转速下的模型进行了数值仿真,并与基于经典薄板理论的假设模态法和有限元方法进行比较分析,验证了本文方法的正确性.仿真结果表明随着柔性板转速的增加,剪切项对悬臂板的动力学行为影响变大,计入了剪切项的本文方法在描述高速旋转板的力学特性时更加精确.对FGM柔性厚板进行数值仿真,仿真结果表明随着功能梯度指数的增加,外侧角点的横向变形和响应周期也随之增大,厚板的固有频率变小,柔性增大,可以根据实际工程需要,调整功能梯度参数以改变结构的力学性能.

## 参　考　文　献


1　Reddy J N. Analysis of functionally graded plates. *International Journal for Numerical Methods in Engineering*, 2000, 47: 663~684

2　仲政, 吴林志, 陈伟球. FGM与结构的若干力学问题研究进展. 力学进展, 2010, 40(5): 528~541(Zhong Z, Wu L Z, Chen W Q. Progress in the study on mechanics problems of functionally graded materials and structures. *Advances in Mechanics*, 2010, 40(5): 528~541(in Chinese))

3　Kane T R, Ryan R R, Banerjee A K. Dynamics of a cantilever beam attached to a moving base. *Journal of Guidance, Control and Dynamics*, 1987, 10(2): 139~151

4　Banerjee A K, Kane T R. Dynamics of a plate in large overall motion. *Journal of Applied Mechanics*, 1989, 56: 887~892

5　刘锦阳, 洪嘉振. 作大范围运动矩形薄板的建模理论和有限元离散方法. 振动工程学报, 2003, 16(2): 175~179(Liu J Y, Hong J Z. Dynamic modeling theory and finite element method for a rectangular plate undergoing large overall motion. *Journal of Vibration Engineering*, 2003, 16(2): 175~179(in Chinese))

6　Boutaghou Z E, Erdman A G, Stolarski H K. Dynamics of flexible beams and plates in large overall motions. *Journal of Applied Mechanics*, 1992, 59(4): 991~999

7 洪嘉振，尤超蓝.刚柔耦合系统动力学研究进展.动力学与控制学报，2004，2(2)：1~6(Hong J Z，You C L. Advances in dynamics of rigid-flexible coupling system. *Journal of Dynamics and Control*，2004，2(2)：1~6(in Chinese))

8 方建士，黎亮，章定国，等.基于刚柔耦合动力学的旋转悬臂梁的频率转向与振型转换特性.机械工程学报，2015，51(17)：59~65(Fang J S，Li L，Zhang D G，et al. Frequency veering and mode shape interaction properties of a rotating cantilever beam based on rigid-flexible coupling dynamics. *Journal of Mechanical Engineering*，2015，51(17)：59~65 ( in Chinese))

9 和兴锁，李雪华，邓峰岩.平面柔性梁的刚-柔耦合动力学特性分析与仿真.物理学报，2011，60(2)：377~382(He X S，Li X H，Deng F Y. Analysis and imitation of dynamic properties for rigid-flexible coupling system of a planar flexible beam. *Acta Physica Sinca*，2011，60(2)：377~382 ( in Chinese))

10 Yoo H H，Chung J. Dynamics of rectangular plates undergoing prescribed overall motion. *Journal of Sound and Vibration*，2001，239(1)：123~137

11 赵飞云，洪嘉振.作大范围运动矩形板的动力学建模理论研究.计算力学学报，2008，25(6)：868~873(Zhao F Y，Hong J Z. Study on dynamic modeling of rectangular plates undergoing large overall motion. *Chinese Journal of Computational Mechanics*，2008，25(6)：868~873(in Chinese))

12 吴根勇，和兴锁，邓峰岩.旋转复合材料板的动力学性能研究.振动与冲击，2008(8)：149~154(Wu G Y，He X S，Deng F Y. Dynamic analysis of a rotating composite plate. *Journal of Vibration and Shock*，2008(8)：149~154(in Chinese))

13 黎亮，章定国，洪嘉振.作大范围运动FGM矩形薄板的动力学特性研究.动力学与控制学报，2013，11(4)：329~335(Li L，Zhang D G，Hong J Z. Dynamics of rectangular functionally graded thin plates undergoing large overall motion. *Journal of Dynamics and Control*，2013，11(4)：329~335(in Chinese))

14 Li L，Zhang D G. Free vibration analysis of rotating functionally graded rectangular plates. *Composite Structures*，2016，136：493~504

15 HashemI S H，Farhadi S，Carra S. Free vibration analysis of rotating thick plates. *Journal of Sound & Vibration*，2009，323：366~384

16 Sudhagar P E，Babu A A，Vasudevan R，et al. Vibration analysis of a tapered laminated thick composite plate with ply drop-offs. *Archive of Applied Mechanics*，2015，85(7)：969~990

17 李坦，齐朝晖，马旭，等. Mindlin板弯曲和振动分析的高阶杂交应力三角形单元.工程力学，2015，32(10)：31~37(Li T，Qi Z H，Ma X，et al. High-order hybrid stress triangular element for mindlin plate bending and vibration analysis. *Engineering Mechanics*，2015，32(10)：31~37 ( in Chinese))

18 Zhang L W，Lei Z X，Liew K M. Free vibration analysis of functionally graded carbon nanotube-reinforced composite triangular plates using the FSDT and element-free IMLS-Ritz method. *Composite Structures*，2015，120：189~199

19 Vu T V，Nguyen N H，Khosravifard A，et al. A simple FSDT-based meshfree method for analysis of functionally graded plates. *Engineering Analysis with Boundary Elements*，2017，79：1~12

20 陈丽华，薛坚，张伟.带边角裂纹悬臂Mindlin板的振动特性研究.动力学与控制学报，2018，16(1)：41~47(Chen L H，Xue J，Zhang W. Study on vibration characteristics of cantilevered mindlin plate with side crack，*Journal of Dynamics and Control*，2018，16(1)：41~47(in Chinese))

21 Yoo H H，Kim S K. Free Vibration Analysis of Rotating Cantilever Plates. *AIAA Journal*，2012，40(11)：2188~2196

# DYNAMIC MODELING AND SIMULATION OF FUNCTIONALLY GRADED MATERIALS PLATES BASED ON FIRST ORDER SHEAR PLATE THEORY *

Yang Xing[1,2†]　Liu Renwei[1]　Hou Peng[1]　Zhang Dingguo[2]

(1.*Shanghai Institute of Spacecraft Equipment*, *Shanghai* 200240, *China*)

(2.*School of Sciences*, *Nanjing University of Science and Technology*, *Nanjing* 210094, *China*)

**Abstract**　The rigid-flexible coupling dynamics of a rectangular functionally graded thick plate undergoing large overall motion was investigated. Based on the first order shear deformation theory, both the transverse shear deformation and the quadratic coupling deformation were taken into account. The rigid-flexible coupling dynamic equations of the functionally graded plate were deduced by Lagrange equations. The finite element method was used to discretize the deformation field with a rectangular element having 20 degrees of freedom based on the classical thin plate theory. The dynamic simulations of the cantilever plate with different rotating speeds were carried out. The influences of function gradient index on the transverse deformation, velocity response frequency and natural frequency of the functionally graded thick plate were also discussed. The results showed that the impact of the shear deformation on structural dynamics becomes notable with an increase in the rotating speed, and the structure is more flexible as the shear deformation is taken into account.

**Key words**　first order shear deformation theory, functional graded material, finite element method, dynamic stiffening

Received 31 May 2019, Revised 31 August 2019.

* The project supported by the National Natural Science Foundation of China (11272155, 11502113) and the Central Special Fund for Operating Expenses of College Basic Research (30917011103)

† Corresponding author E-mail: 115113001212@njust.edu.cn